Journal of Computational Mathematics
Vol.29, No.5, 2011, 491–500.

http://www.global-sci.org/jcm
doi:10.4208/jcm.1105-m3392

A HIGH ORDER ADAPTIVE FINITE ELEMENT METHOD FOR SOLVING NONLINEAR HYPERBOLIC CONSERVATION LAWS*

Zhengfu Xu
Department of Mathematics, Michigan State University, East Lansing, MI 48824, USA
Email: zhengfu@math.msu.edu
Jinchao Xu
Department of Mathematics, Pennsylvania State University, University Park, PA 16802, USA
Email: xu@math.psu.edu
Chi-Wang Shu
Division of Applied Mathematics, Brown University, Providence, RI 02912, USA
Email: shu@dam.brown.edu

Abstract

In this note, we apply the h-adaptive streamline diffusion finite element method with a small mesh-dependent artificial viscosity to solve nonlinear hyperbolic partial differential equations, with the objective of achieving high order accuracy and mesh efficiency. We compute the numerical solution to a steady state Burgers equation and the solution to a converging-diverging nozzle problem. The computational results verify that, by suitably choosing the artificial viscosity coefficient and applying the adaptive strategy based on *a posterior* error estimate by Johnson *et al.*, an order of $N^{-3/2}$ accuracy can be obtained when continuous piecewise linear elements are used, where N is the number of elements.

Mathematics subject classification: 65N30.
Key words: Adaptive finite element, Nonlinear hyperbolic conservation law.

1. Introduction

For the nonlinear hyperbolic equations

$$u_t + f(u)_x = 0 \tag{1.1}$$

discontinuities may develop after finite time despite the regularity of the initial condition. This accounts for most of the difficulties in the design of numerical schemes to solve the nonlinear hyperbolic equation (1.1) accurately. It has been shown [6, 7] that the numerical solution generated by high order methods produces in general only first order accuracy for pointwise errors, because the information carried along characteristics is degraded to first order when passing through the discontinuity. Much work has been done in the literature to achieve high order accuracy in the presence of discontinuities. To name a few, pre- and post-processing has been introduced in [6,7] to recover high order pointwise accuracy for linear hyperbolic systems; Glimm and his co-authors [2] have designed high order front tracking algorithms; Gottlieb et al. [3] applied the Gegenbauer postprocessing to recover the designed accuracy up to the shock front in the framework of high order weighted essentially non-oscillatory (WENO) schemes. In

* Received April 21, 2010 / Revised version received September 24, 2010 / Accepted May 13, 2011 / Published online September 9, 2011 /

this note, we study an h-adaptive finite element method for solving (1.1) with a mesh dependent artificial viscosity

$$u_t + f(u)_x = \varepsilon u_{xx}, \tag{1.2}$$

where ε is suitably chosen together with an h-adaptivity strategy to enhance accuracy. An advantage of this approach is that the solution is regularized by an artificial viscosity and the entropy condition should be satisfied within this framework. However, one main question in this approach is whether we can solve (1.2) accurately and efficiently with a sharp viscous shock layer existing in the solution when ε diminishes with the mesh size. Or equivalently, can we resolve the sharp layer while keeping the overall error small. These questions will be addressed by using an adaptive mechanism to adjust grid distribution automatically with mesh refinement in regions where small scale features (such as shock layers and vortex sheets) exist.

Adaptive finite element methods have been extensively studied and applied for solving linear parabolic partial differential equations [1,4], and also explored for nonlinear hyperbolic conservation laws [5]. This approach is efficient for solving problems whose solutions contain multiple features. One important class of adaptive strategies is based on the measurement of the residual with certain norm. The underlying mesh is adjusted locally to obtain an even distribution of the *a posterior* error or a reduction of the overall error.

The computation in this note is based on the *a posterior* error estimation of Johnson and Szepessy [5]. In their work, they provided the *a posterior* error estimates for $\varepsilon = CN^{-1}$, where N is the total number of elements, in the following form

$$||e|| \leq C^s C^i \left\| \frac{h^2}{\varepsilon} R(U) \right\|. \tag{1.3}$$

Here and below, the unmarked norm is the L^2-norm, $e = u - U$, where u is the exact solution of (1.1) and U is the finite element numerical solution of (1.2). $R(U) = U_t + f(U)_x - \varepsilon U_{xx}$ is the residual of the finite element solution U (evaluated appropriately). C^s is the stability constant and C^i is the interpolation constant, which depends only on the degree of the polynomials and the shape of the finite elements. It should also be noted that C^s depends on both the analytic and numerical solutions of the underlying differential equation. Therefore, strictly speaking the above estimate is not a usual *a posterior* error estimate which should only depend on U and h. As commented in [5], C^s is in general a moderate number. Analytic estimation of C^s is restricted to certain model cases only, where the system is strictly hyperbolic in one dimension allowing the presence of weak shocks, noninteracting shocks and rarefaction waves. In general, it is reasonable and realistic to estimate the bound of C^s computationally. We refer to [5] for the details. It is suggested in [5] that adaption of the grids could be carried out based on this *a posterior* error estimate, but it remains unclear what accuracy can be achieved by adapting the mesh based on this estimation, theoretically or numerically. Our computation in this note indicates that an order of $N^{-3/2}$ can be achieved for the two benchmark problems in scalar and system cases.

2. Numerical Results

The adaptive strategy here is that the mesh is adapted in an iterative way in order to get equal or close to equal amount of $||\frac{h^2}{\varepsilon}R(U)||$ on each element. A threshold is set to stop the iteration when the change of the total residue $||\frac{h^2}{\varepsilon}R(U)||$ is stagnant. The test problems here are the model cases we mentioned above, where the bound of stability constant C^s could be

analytically estimated. To be precise, we intend to choose the proper parameter ε together with the above adaptive strategy which gives the best accurate numerical solution. The choice of ε is delicate in the sense that the solution of (1.2) is closer to solution of (1.1) for smaller ε. However, given a fixed number of grids, there might not be enough grid points to be moved into the sharp layer for too small ε without affecting errors elsewhere. Intuitively, to balance the choice of ε, we should consider that

$$||u - U|| \leq ||u - u_\varepsilon|| + ||u_\varepsilon - U|| \leq c\varepsilon \log(\varepsilon) + ||u_\varepsilon - U||.$$

The choice of a smaller ε will make the first term small, however the second term could become larger because it is more difficult to approximate such u_ε, which contains sharp layers, with the given number of mesh points. In order to obtain accuracy of order $\mathcal{O}(N^{-m})$, we need ε to be smaller than $\mathcal{O}(N^{-m})$. We will perform numerical experiment to guide the choice of the "optimal" ε in (1.2), in relation to the number of elements N, and to determine the accuracy achieved by the adaptive method with this optimal ε. It seems from our numerical results that $m > 1.5$ can be achieved. From now on, we will focus on steady state nonlinear hyperbolic problem

$$f(u)_x = 0, \tag{2.1}$$

and its viscous counterpart

$$f(u)_x = \varepsilon u_{xx}. \tag{2.2}$$

The generalization to time dependent problems is nontrivial considering the moving shock front which demands extra attention and probably a different approach.

In the following numerical experiments, for each fixed grid number N, we perform an adaptive computation for a series of decreasing values of ε. For the largest value of ε, we start the iteration of mesh movement with a uniformly distributed grid $x_0 = a$, $x_i = x_0 + i\frac{b-a}{N}$, $i = 1, 2 \cdots, N$. For the remaining values of ε, we start the iteration of mesh movement with the final mesh of the previous larger value of ε. In the following, we list the steps of the adaptive algorithm to move the mesh points for solving (2.2).

The algorithm flowchart

- **Step 1:** Based on the grid x_i, $i = 0, 1, \cdots, N$, we solve the problem (2.2) with the piecewise linear streamline diffusion finite element method. The resulting nonlinear equation is solved by a Newton-GMRES plus back-track loop iteration method.
- **Step 2:** We compute the total residue $||\frac{h^2}{\varepsilon}R(U)||$. If the change of $||\frac{h^2}{\varepsilon}R(U)||$ is smaller than the preset threshold $\tau = 10^{-8}$, the mesh movement is finished and we compute and document the error in the table. Otherwise we move to the next step.
- **Step 3:** We redistribute the grid such that the mesh size

$$h_i = \frac{r_i}{\sum r_i}, \qquad r_i = \frac{1}{0.5||\frac{h^2}{\varepsilon}R(U)||_{k_i} + 0.5\lambda},$$

where k_i is the i-th cell and $\lambda = ||\frac{h^2}{\varepsilon}R(U)||$. This step is attempting to have a smaller mesh size when the local residue is larger. We then interpolate the numerical solution U on the new grid from previously computed solution as initial guess of the Newton-GMRES solver and move to Step 1.

Test Problem 1. We show the result for the steady state Burgers equation

$$\left(\frac{u^2}{2}\right)_x = 0 \tag{2.3}$$

as a limit, when $\varepsilon \to 0$, of the viscous Burgers equation

$$\left(\frac{u^2}{2}\right)_x = \varepsilon u_{xx}. \tag{2.4}$$

The computational domain is $[0, 1]$. Dirichlet boundary condition is imposed as $u(0) = a$, $u(1) = b$. This is an important test problem for many numerical methods in computational fluid dynamics. It has a unique, monotone, symmetric solution

$$u = -m \tanh\left(\frac{m(x - 0.5)}{2\varepsilon}\right), \tag{2.5}$$

where m is decided by values of the solution at boundary. After applying the test function $v + chJ(u)v_x$, where $J(u) = u$ is the Jacobian of the flux $f(u) = u^2/2$ and h is the local element size, to Eq. (2.4), we obtain the weak form

$$-\int \frac{u^2}{2} v_x dx + \int \left(\frac{u^2}{2}\right)_x chuv_x dx + \varepsilon \int u_x v_x dx - \varepsilon \int u_{xx} chuv_x dx = 0, \tag{2.6}$$

in which the second term in the test function accounts for the least square stabilizer. Here and below, we approximate the integrals through the trapezoidal formula

$$\int_{x_i}^{x_{i+1}} f(x)dx \approx \frac{h}{2}\big(f(x_i) + f(x_{i+1})\big).$$

Table 2.1: $||u - U||_{L^1}$ for Test Problem 1.

	L^1 error for N number of elements				
ε	$N = 80$	$N = 160$	$N = 240$	$N = 320$	$N = 480$
8.00e-2	2.17e-1	2.17e-1	2.17e-1	2.17e-1	2.17e-1
4.00e-2	1.10e-1	1.10e-1	1.10e-1	1.10e-1	1.10e-1
2.00e-2	5.54e-2	5.54e-2	5.54e-2	5.54e-2	5.54e-2
1.00e-2	2.77e-2	2.77e-2	2.77e-2	2.77e-2	2.77e-2
5.00e-3	1.39e-2	1.38e-2	1.38e-2	1.38e-2	1.38e-2
2.50e-3	6.99e-3	6.94e-3	6.93e-3	6.93e-3	6.93e-3
1.25e-3	3.51e-3	3.48e-3	3.47e-3	3.47e-3	3.46e-3
6.25e-4	1.76e-3	1.76e-3	1.74e-3	1.73e-3	1.73e-3
3.125e-4	8.89e-4	8.84e-4	8.77e-4	8.72e-4	8.73e-4
1.5625e-4	4.45e-4	4.40e-4	4.38e-4	4.36e-4	4.36e-4
7.8125e-5	2.23e-4	2.21e-4	2.18e-4	2.20e-4	2.17e-4
3.90625e-5	1.14e-4	1.12e-4	1.09e-4	1.12e-4	1.09e-4
1.953125e-5	6.26e-5	5.88e-5	5.47e-5	6.05e-5	5.56e-5
9.765625e-6	4.13e-5	3.54e-5	2.74e-5	3.84e-5	2.94e-5
4.8828125e-6	3.52e-5	2.72e-5	1.37e-5	3.15e-5	1.77e-5
2.44140625e-6	3.51e-5	2.55e-5	6.93e-6	3.06e-5	1.37e-5
1.220703125e-6	3.51e-5	**2.53e-5**	3.60e-6	**3.05e-5**	1.30e-5
6.103515625e-7	**3.50e-5**	2.54e-5	2.03e-6	3.05e-5	**1.29e-5**
3.0517578125e-7	3.51e-5	2.54e-5	1.44e-6	3.05e-5	1.29e-5
1.52587890625e-7	3.51e-5	2.54e-5	**1.30e-6**	3.05e-5	1.29e-5

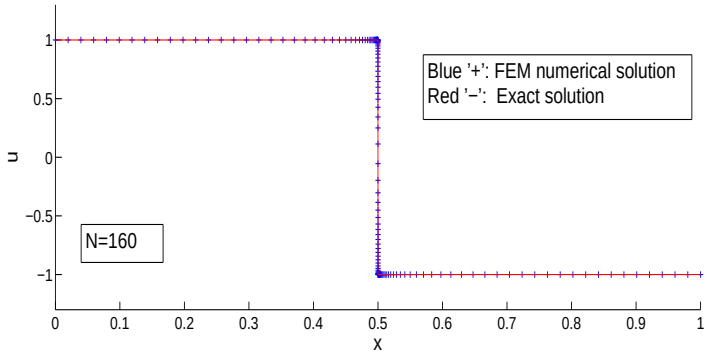

Fig. 2.1. Solution to Test Problem 1: resolution of shock.

Both the trial function u and the test function v are chosen as continuous piecewise linear functions on $[0,1]$. The resulting nonlinear equation from the discretization of the weak form is solved by the Newton-GMRES plus back-track loop method. The solution for bigger ε is used as the initial guess of the Newton iteration for smaller ε. All the integrals are evaluated element-wise, therefore

$$\int u_{xx} chuv_x dx = 0$$

for piecewise linear elements. To compute $||\frac{h^2}{\varepsilon}R(U)||$, we need to reconstruct U by performing a quadratic spline interpolation given the computed piecewise linear solution. In Table 2.1, we choose five different numbers N of total elements, and compare the computed solution with the exact solution of (2.3), using different choices of the artificial viscosity ε. The best accuracy that can be achieved for each fixed number of mesh elements N when varying ε is denoted by boldface. The empty spaces in the table imply that the iterative procedure to obtain the numerical solution does not produce more accurate solution or fails to converge while reducing ε. It can be seen clearly that for this very simple problem (piecewise constant exact solution with one discontinuity), the smaller the artificial viscosity coefficient ε, the smaller the L^1 error. This is not surprising since the optimal grid distribution strategy is to cluster as many points near the shock as possible. The numerical solution as well as the grid distribution for the optimal choice of ε when $N = 160$ can be seen in Fig. 2.1. We can clearly see the severe concentration of points towards the shock location.

Test Problem 2. The second example is the Burgers equation with a source term

$$\left(\frac{u^2}{2}\right)_x = a(x)u, \quad 0 \le x \le 1 \tag{2.7}$$

with $a(x) = 2x - 3$, $u(0) = 1$, $u(1) = -2$. The boundary value problem has a steady state solution:

$$u(x) = \begin{cases} x^2 - 3x + 1, & x < \dfrac{3-\sqrt{7}}{2}, \\ x^2 - 3x, & x \ge \dfrac{3-\sqrt{7}}{2}. \end{cases} \tag{2.8}$$

Here $x = (3 - \sqrt{7})/2$ is the shock location, obtained by the Rankine-Hugoniot jump condition.

After adding artificial viscosity to (2.7), we have the viscous equation

$$\left(\frac{u^2}{2}\right)_x = a(x)u + \varepsilon u_{xx}, \quad 0 \le x \le 1. \tag{2.9}$$

In Table 2.2, we choose five different numbers N of total elements, and compare the computed solution of (2.9) with the exact solution of (2.7) using different choices of the artificial viscosity ε. The "optimal" choice of ε, which gives the smallest error for each N, is again shown in bold face in Table 2.2. The empty spaces in the table still imply that the error of numerical

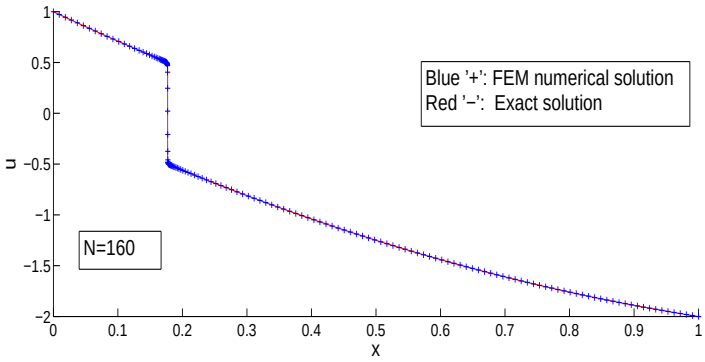

Fig. 2.2. Solution to Test Problem 2: resolution of shock.

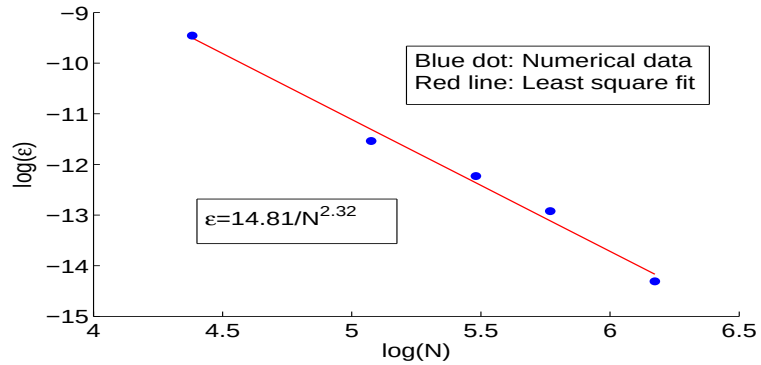

Fig. 2.3. Test Problem 2: ε versus N and a least square fit.

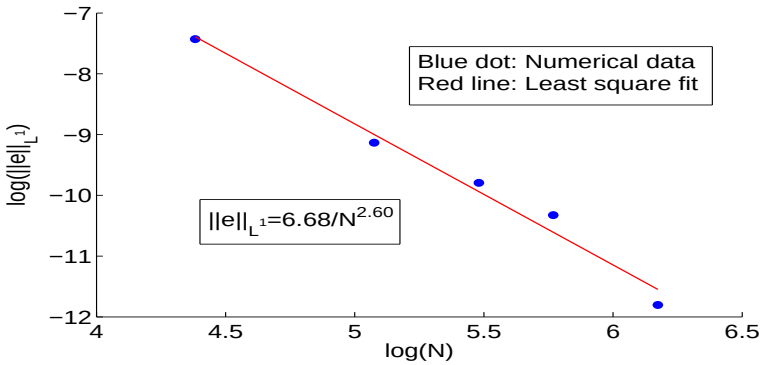

Fig. 2.4. Test Problem 2: $||e||_{L^1}$ versus N and a least square fit.

approximation can not be reduced by simply diminishing viscosity subject to convergence of the iterative procedure. The numerical solution as well as the grid distribution for the optimal choice of ε when $N = 160$ can be seen in Fig. 2.2. We can still see a concentration of points towards the shock location, although this concentration is less severe than in the previous test case.

We plot the optimal ε versus N in Fig. 2.3, which shows a pattern of $\varepsilon = C/N^r$ by a least square fit (the solid line in Fig. 2.3) with $C = 6.68$ and $r = 2.60$. In Fig. 2.4, the L^1 error versus N is shown, when the optimal ε is used. A least square fit (the solid line in Fig. 2.4) shows that the error has the pattern $||e||_{L^1} = C/N^r$ with $C = 14.81$ and $r = 2.31$.

Table 2.2: $||u - U||_{L^1}$ for Test Problem 2.

	Number of elements				
ε	$N = 80$	$N = 160$	$N = 240$	$N = 320$	$N = 480$
8.00e-2	1.28e-1	1.28e-1	1.28e-1	1.28e-1	1.28e-1
4.00e-2	7.90e-2	7.88e-2	7.88e-2	7.88e-2	7.88e-2
2.00e-2	4.69e-2	4.67e-2	4.66e-2	4.66e-2	4.65e-2
1.00e-2	2.63e-2	2.63e-2	2.63e-2	2.63e-2	2.63e-2
5.00e-3	1.47e-2	1.44e-2	1.44e-2	1.44e-2	1.43e-2
2.50e-3	8.10e-3	7.65e-3	7.61e-3	7.62e-3	7.61e-3
1.25e-3	4.04e-3	3.99e-3	3.93e-3	3.94e-3	3.93e-3
6.25e-4	2.29e-3	2.07e-3	2.00e-3	2.00e-3	2.00e-3
3.125e-4	1.45e-3	1.10e-3	1.01e-3	1.01e-3	1.01e-3
1.5625e-4	6.75e-4	6.15e-4	5.10e-4	5.06e-4	5.13e-4
7.8125e-5	**5.49e-4**	3.71e-4	2.63e-4	2.55e-4	2.62e-4
3.90625e-5	7.00e-4	2.57e-4	1.39e-4	1.31e-4	1.39e-4
1.953125e-5		1.53e-4	8.07e-5	7.14e-5	8.21e-5
9.765625e-6		**1.08e-4**	5.71e-5	4.49e-5	3.17e-5
4.8828125e-6		1.12e-4	**5.58e-5**	3.36e-5	1.85e-5
2.44140625e-6			6.06e-5	**3.28e-5**	1.19e-5
1.220703125e-6				3.52e-5	8.62e-6
6.103515625e-7					**7.48e-6**
3.0517578125e-7					7.55e-6

Test Problem 3. We consider the quasi-one-dimensional converging-diverging nozzle flow. The governing equations are the usual Euler system with a source term:

$$\mathbf{u}_t + f(\mathbf{u})_x = -\frac{a'(x)}{a(x)} g(\mathbf{u}) \tag{2.10}$$

with

$$\mathbf{u} = \begin{pmatrix} \rho \\ \rho u \\ E \end{pmatrix}, \qquad f(\mathbf{u}) = \begin{pmatrix} \rho u \\ \rho u^2 + P \\ (E+P)u \end{pmatrix}, \qquad g(\mathbf{u}) = \begin{pmatrix} \rho u \\ \rho u^2 \\ (E+P)u \end{pmatrix},$$

where ρ, u, P and E are the density, velocity, pressure and total energy respectively, and $a(x)$ describes the cross area of the nozzle. The shape of the nozzle is calculated by requiring linear distribution of the Mach number from $M = 0.8$ at the inlet to $M = 1.8$ at the exit assuming the flow is isentropic and fully expanded. The equation of the state is $P = (\gamma -$

$1)(E - \frac{1}{2}\rho u^2)$ with $\gamma = 1.4$. We compute the solution on the domain $[0, 1]$ with the Dirichlet boundary condition: at $x = 0$, $(\rho, u, p) = (0.7399925, 0.8912498, 0.6560218)$; at $x = 1$, $(\rho, u, p) = (0.8803624, 0.5405094, 0.8436197)$. Those are the values of the exact solution to the equation (2.10). The viscous version of (2.10) takes the form

$$\mathbf{u}_t + f(\mathbf{u})_x = -\frac{a'(x)}{a(x)} g(\mathbf{u}) + \varepsilon \mathbf{u}_{xx}. \tag{2.11}$$

By applying the test function, at steady state, the weak form follows as

$$-\int f(\mathbf{u})\mathbf{v}_x dx + \int f(\mathbf{u})_x chJ(\mathbf{u})\mathbf{v}_x dx + \int \frac{a'(x)}{a(x)} g(\mathbf{u})(\mathbf{v} + chJ(\mathbf{u})\mathbf{v}_x) dx + \varepsilon \int \mathbf{u}_x \mathbf{v}_x dx - \varepsilon \int \mathbf{u}_{xx} chJ(\mathbf{u})\mathbf{v}_x dx = 0,$$

with added streamline diffusion, where $J(\mathbf{u})$ is the Jacobian matrix. Once again, since the integral $\varepsilon \int \mathbf{u}_{xx} chJ(\mathbf{u})\mathbf{v}_x dx$ is evaluated on each cell, it is 0 for piecewise linear elements. The weak form will then be

$$-\int f(\mathbf{u})\mathbf{v}_x dx + \int f(\mathbf{u})_x chJ(\mathbf{u})\mathbf{v}_x dx + \int \frac{a'(x)}{a(x)} g(\mathbf{u})(\mathbf{v} + chJ(\mathbf{u})\mathbf{v}_x) dx + \varepsilon \int \mathbf{u}_x \mathbf{v}_x dx = 0.$$

Again, in Table 2.3, we choose five different numbers N of total elements, and compare the computed solution of (2.11) with the exact solution of (2.10) using different choices of the artificial viscosity ε. The "optimal" choice of ε, which gives the smallest error for each N, is shown in bold face in the table. The empty spaces in the table still imply that the iterative procedure to obtain the numerical solution does not produce better accuracy or fails to converge while reducing viscosity. The numerical solution as well as the grid distribution for the optimal choice of ε when $N = 160$ can be seen in Fig. 2.5. The concentration of points towards the shock location is less severe.

We plot the optimal ε versus N in Fig. 2.6, which shows a pattern of $\varepsilon = CN^{-r}$ by a least square fit (the solid line in Fig. 2.6) with $C = 0.38$ and $r = 1.50$. In Fig. 2.7, the L^1 error

Table 2.3: $||u - U||_{L^1}$ for Test Problem 3.

	Number of elements				
ε	$N = 80$	$N = 160$	$N = 240$	$N = 320$	$N = 480$
8.00e-2	2.98e-1	2.98e-1	2.98e-1	2.98e-1	2.98e-1
4.00e-2	2.32e-1	2.32e-1	2.32e-1	2.32e-1	2.32e-1
2.00e-2	1.76e-1	1.76e-1	1.76e-1	1.76e-1	1.76e-1
1.00e-2	1.18e-1	1.18e-1	1.18e-1	1.18e-1	1.18e-1
5.00e-3	5.76e-2	5.75e-2	5.75e-2	5.75e-2	5.75e-2
2.50e-3	2.69e-2	2.69e-2	2.69e-2	2.69e-2	2.69e-2
1.25e-3	1.31e-2	1.31e-2	1.31e-2	1.31e-2	1.31e-2
6.25e-4	**6.63e-3**	6.51e-3	6.52e-3	6.51e-3	6.51e-3
3.125e-4	7.05e-3	3.28e-3	3.24e-3	3.24e-3	3.24e-3
1.5625e-4		**1.72e-3**	1.62e-3	1.61e-3	1.61e-3
7.8125e-5		2.18e-3	**9.47e-4**	**8.19e-4**	8.08e-4
3.90625e-5			1.21e-3	9.26e-4	**4.10e-4**
1.953125e-5					4.62e-4

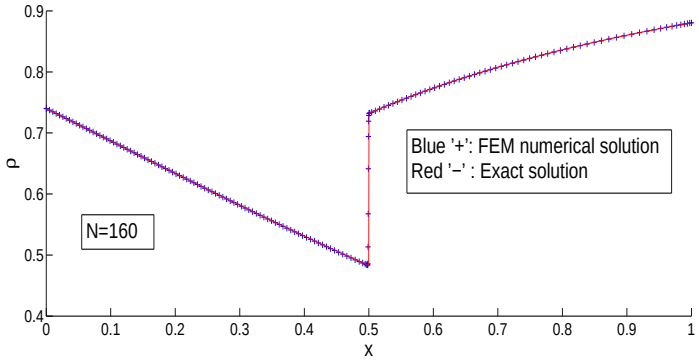

Fig. 2.5. Solution to Test Problem 3: resolution of shock.

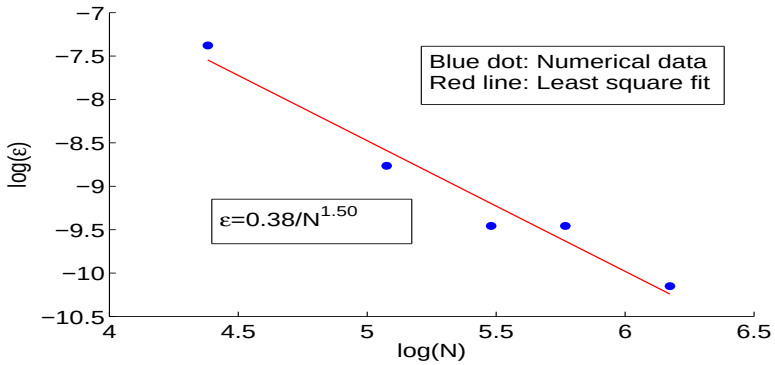

Fig. 2.6. Test Problem 3: ϵ versus N and a least square fit.

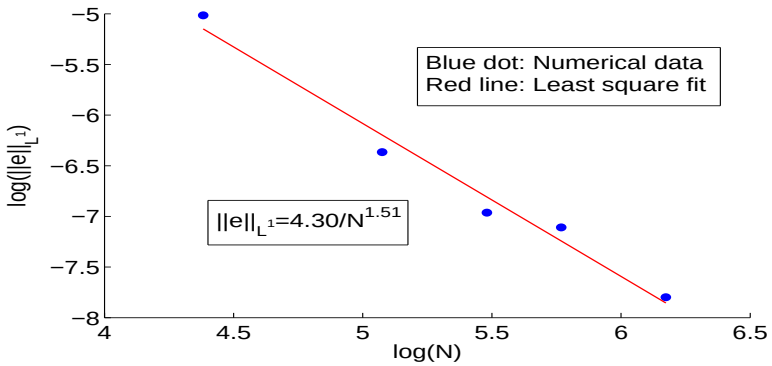

Fig. 2.7. Test Problem 3: $||e||_{L^1}$ versus N and a least square fit.

versus N is shown, when the optimal ε is used. A least square fit (the solid line in Fig. 2.7) shows that the error has the pattern $||e||_{L^1} = CN^{-r}$ with $C = 4.30$ and $r = 1.51$.

The last two examples seem to show that we should choose the artificial viscosity coefficient ε as small as possible for each fixed mesh size N, subject to the convergence of the iterative procedure to obtain the numerical solution, and the final L^1 error of the numerical solution can achieve at least $N^{-3/2}$ order of accuracy through adapting mesh based on the estimate (1.3). It is also worth to point out that the amount of viscosity ε that we use to obtain $\mathcal{O}(N^{-3/2})$ or better order of accuracy, which is around $\varepsilon = \mathcal{O}(N^{-3/2})$, is already out of the valid range

($\varepsilon \geq CN^{-1}$) that the *a posterior* error estimation (1.3) holds, as analyzed in [5].

We remark that we have used piecewise linear finite elements in this paper to simplify the computation. Higher order finite elements can also be used in the same framework, however, accuracy is not expected to improve beyond second order since we are measuring the global error including the shocks. It is possible to obtain better accuracy away from the shock front by using high order elements, but this is not the purpose of our study. It should be made clear that the guideline we provide here is purely numerical due to the essential difficulty of the nonlinear problem. The results in this paper serve as only numerical proof that high order accuracy can be obtained with suitably chosen parameters and proper adaptive strategy. We indeed observe the pattern of the optimal $\varepsilon = cN^{-m}$ with $m > 1.5$, and global L^1 error smaller than cN^{-m} with $m > 1.5$. This indicates the potential of adaptive finite element methods for shocked problems in obtaining higher than first order global convergence.

Acknowledgments. The research of the second author was supported by DMS-0915153 and DMS-0749202. The research of the third author was supported by AFOSR grant FA9550-09-1-0126 and NSF grant DMS-0809086.

References

[1] I. Babuska and W.C. Rheinboldt, A-posteriori error estimates for the finite element method, *Int. J. Numer. Meth. Eng.*, **12** (2005), 1597-1615.

[2] J. Glimm, X. Li, Y. Liu, Z. Xu and N. Zhao, Conservative front tracking with improved accuracy, *SIAM J. Numer. Anal.*, **41** (2003), 1926-1947.

[3] S. Gottlieb, D. Gottlieb and C.-W. Shu, Recovering high-order accuracy in WENO computations of steady-state hyperbolic systems, *J. Sci. Comput.*, **28** (2006), 307-318.

[4] C. Johnson and K. Errickson, Adaptive finite element methods for parabolic problems I: a linear model problem, *SIAM J. Numer. Anal.*, **28** (1991), 43-77.

[5] C. Johnson and A. Szepessy, Adaptive finite element methods for conservation laws based on a posteriori error estimates, *Commun. Pur. Appl. Math.*, **48** (1995), 199-234.

[6] A. Majda and S. Osher, Propagation of error into regions of smoothness for accurate difference approximations to hyperbolic equations, *Commun. Pur. Appl. Math.*, **30** (1977), 671-705.

[7] M.S. Mock and P.D. Lax, The computation of discontinuous solutions of linear hyperbolic equations, *Commun. Pur. Appl. math.*, **31** (1978), 423-430.